

Effect of Haptic-Interface Virtual Kinematics on the Performance and Preference of Novice Users in Telemanipulated Retinal Surgery

Manikantan Nambi, Paul S. Bernstein, and Jake J. Abbott

Abstract—Telemanipulated robot-assisted surgical procedures of the retina require precise manipulation of instruments inserted through trocars in the sclera. However, there is not a unique mapping of the motions of the surgeon's hand to the lower-dimensional motions of the instrument through the trocar, and it is not obvious what method would be best. In this letter, we study operator performance during a precision positioning task reminiscent of telemanipulated retinal surgery on a force-sensing phantom retina with three viable and previously considered options for the haptic-interface kinematics. The haptic-interface kinematics are implemented virtually, in software, on a PHANTOM Premium 6DOF haptic interface. Results from a study with 12 novice human subjects show that overall performance is best with the kinematics that represent a compact and inexpensive option, and that subjects' subjective preference agrees with the objective performance results.

Index Terms—Haptics and Haptic Interfaces, Human Factors and Human-in-the-Loop, Medical Robots and Systems.

I. INTRODUCTION

MINIMALLY invasive surgical procedures of the retina—including peeling of membranes, repair of retinal tears, and cannulation of blood vessels—involves inserting instruments into the eye through trocars on the sclera (Fig. 1). Surgeons must pivot the instruments about the trocars to reduce excessive stress on the scleral tissue, and reduce unwanted eye motion for stable visualization. With these instruments, surgeons manipulate delicate structures that can range from less than one micrometer to a few hundred micrometers [1]. Procedures like membrane peeling require delicate and precise motions of the instruments by the surgeon. For example, scraping membranes with a diamond-dusted scraper requires motions similar to painting with a brush, with contact forces that should be kept to a minimum. Grasping the membrane and peeling it with a forceps requires slow controlled movements just above the surface of the retina to reduce fragmentation of

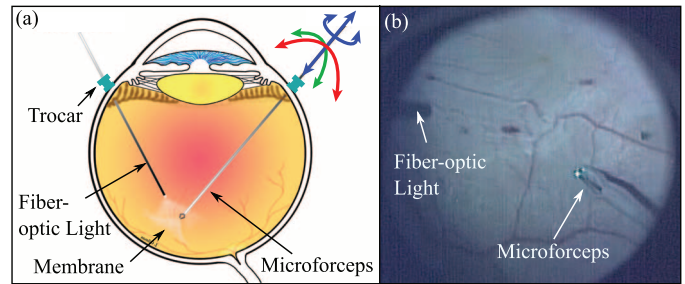


Fig. 1. (a) Illustration of membrane-peeling surgery. Surgeons use a combination of three rotary and one translational motions of the instrument to achieve the desired instrument motion inside the eye while trying to maintain the trocar point stationary. Modified version of image courtesy of James Gilman, CRA, FOPS. (b) Membrane-peeling surgery as seen through a surgical microscope. Image courtesy of Nikhil Batra, M.D.

the membrane. The curvature of the retina poses a challenge to the surgeon, especially to inexperienced surgeons who often fail to compensate for the curvature. In other experimental procedures like retinal vein cannulation, the surgeon has to first precisely position a needle close to a retinal vein, followed by a delicate motion along a straight line to insert the needle into the vein. To perform the complex motions required in retinal surgery, surgeons use a combination of rotary and linear motions of the hand and wrist to achieve the desired end-effector motion while trying to minimize motion at the trocar. As a result, retinal-surgical procedures are difficult and take years of training to master.

To improve surgical outcomes in retinal surgery, a number of research groups have developed robot-assisted retinal-surgery systems—including both telemanipulated systems [2]–[8], and cooperative manipulators [9], [10] that could be used in a telemanipulated approach—which have been shown to improve positioning precision in retinal procedures. There are two primary potential benefits that motivate telemanipulated surgical systems relative to both manual surgery and cooperative manipulators. The first is the ability to scale down the motion of the surgeon's hand to improve precision, which can be combined with filtering for additional tremor reduction [10]. The second is the ability to provide “intuitive” control directly over the end-effector of the instrument, as opposed to controlling the less-intuitive inverted motion of the instrument's handle. This potential benefit is motivated by the intuitive nature of robotic systems such as the da Vinci Surgical System compared to manual laparoscopic surgery. However, as we show in this letter, how to implement intuitive control of the end-effector is not

Manuscript received August 30, 2015; accepted January 29, 2016. Date of publication February 29, 2016; date of current version April 11, 2016. This paper was recommended for publication by Associate Editor M. A. Otaduy and Editor A. Bicchi upon evaluation of the reviewers comments. This work was supported by the Intuitive Surgical Technology Research Grants.

M. Nambi is with the Energid Technologies, Cambridge, MA 02138 USA (e-mail: m.nambi@utah.edu).

P. S. Bernstein is with the Moran Eye Center, Department of Ophthalmology and Visual Sciences, University of Utah, Salt Lake City, UT 84132 USA (e-mail: paul.bernstein@hsc.utah.edu).

J. J. Abbott is with the Department of Mechanical Engineering, University of Utah, Salt Lake City, UT 84112 USA (e-mail: jake.abbott@utah.edu).

Digital Object Identifier 10.1109/LRA.2016.2535980

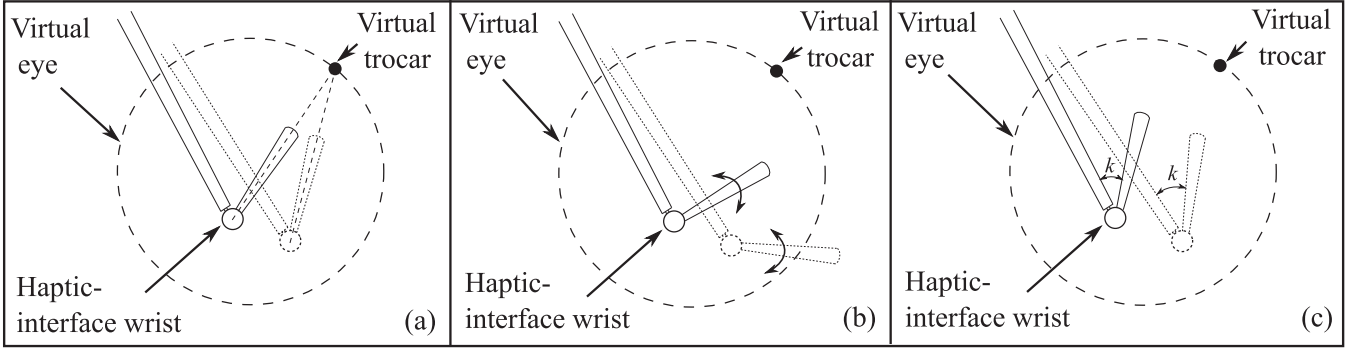


Fig. 2. Orientation of the haptic-interface stylus with different haptic-interface kinematics. In each image, the haptic-interaction point (i.e., the wrist of the stylus) that is mapped to the telemanipulated instrument end-effector is shown in the same two locations, but the behavior of the stylus held by the user depends on the virtual kinematics implemented. (a) 4-DOF Virtual Trocar: The orientation of the stylus matches the orientation of the instrument inside the eye. (b) 6-DOF Underactuated: The users are free to orient the stylus as they like. (c) 4-DOF Separable: The orientation of the stylus is a fixed constant value (k) with respect to the haptic interface.

trivial, and a recent study suggests that we should not automatically assume that telemanipulated retinal-surgery systems are more intuitive than cooperative manipulators [10].

The trocar constrains the instrument to a point on the surface of the eye, kinematically removing two degrees-of-freedom (2-DOF), leaving only 4-DOF to define the pose of the instrument. These 4-DOF include the 3-DOF orientation about the center of the trocar, typically controlled using a remote-center-of-motion (RCM) mechanism [9] or a “virtual RCM” implemented in software, and an additional 1-DOF translation through the trocar, as depicted in Fig. 1. For intuitive telemanipulation of the instrument’s end-effector, these less-than-intuitive 4-DOF are uniquely mapped from the more-intuitive 3-DOF Cartesian position of the end-effector and 1-DOF rotation of the instrument’s shaft. (Note that this is true of rigid instruments, but it is not the case when using “intra-ocular dexterity” devices [3].) The precise manipulators used for retinal surgery typically have limits on achievable velocity relative to achievable velocity of the human hand, so it is typically desirable to utilize a haptic interface that has, at a minimum, actuation in the 3-DOF Cartesian position to convey the instrument’s constrained velocity to the surgeon. However, there is not a unique “correct” mapping from the 6-DOF pose of the surgeon’s hand to the 4-DOF pose of the end-effector. As a result, different research groups have utilized different haptic-interface kinematics in their respective telemanipulation systems; these choices have typically been made with some rationale, but without rigorous justification.

In this letter, we study operator performance on a positioning task that simulates typical motions used in retinal surgery, using three viable haptic-interface kinematics introduced in previous studies. The retinal-surgery manipulator introduced in [8] is used in the experiments, and the different haptic-interface kinematics are implemented virtually, in software, on a PHANTOM Premium 6DOF haptic interface. We present results from an experiment with 12 novice human subjects, using a variety of performance metrics designed to quantify the subjects’ ability to perform precise and efficient motions. By utilizing novice subjects with no prior familiarity with retinal surgery, our study investigates which haptic-interface kinematics lead to the best

performance and are most preferred by users that have no pre-existing bias due to training. The conclusion of our study is that the haptic-interface kinematics that represent the simplest, most-compact, and least-expensive option lead to the best overall performance and are also subjectively most preferred. We also provide discussion with caveats to this conclusion. The determination of which haptic-interface kinematics are superior for experienced retinal surgeons, either with or without additional training, is left as an open question.

II. HAPTIC-INTERFACE KINEMATICS

The three previously introduced haptic-interface kinematics that we consider in this letter are as follows.

A. 4-DOF Virtual Trocar

This type of kinematics constrains the haptic interface to have the same kinematic constraints as the instrument passing through the trocar, but with the user effectively holding a location on the instrument that is below the trocar rather than above it (as in manual surgery). As the 3-DOF position of the end-effector and 1-DOF rotation about the instrument’s shaft axis are controlled, the 2-DOF orientation of the haptic interface’s stylus matches the orientation of the instrument through the trocar, effectively creating a virtual trocar in the haptic interface’s workspace, as shown in Fig. 2(a). The potential benefit of this type of haptic-interface kinematics is that there is always a one-to-one mapping between motions of the haptic interface and motions of the instrument, and there is always a direct correspondence between the pose of the stylus in the surgeon’s hand and the instrument being observed in the microscope.

There are two methods to implement the 4-DOF Virtual Trocar kinematics: mechanically or in software. The systems in [7] and [11] use the mechanical approach, building custom haptic interfaces with the correct degrees of freedom. The kinematics can also be implemented in software using a haptic interface with 6-DOF actuation, creating a virtual mechanism to which the haptic interface’s stylus is bound using impedance control (as we do in this letter). In the virtual-mechanism

approach, the kinematics can be accomplished invariant to scaling, since the location of the virtual trocar can be placed arbitrarily relative to the stylus. In the mechanical approach, to correctly implement scaling, a prismatic degree of freedom must be implemented to effectively lengthen the stylus relative to the mechanical trocar point; this approach has been implemented in prior works.

We originally hypothesized that the 4-DOF Virtual Trocar kinematics would be the best option, due to the close correspondence between the master and the slave. However, as we will show, the results of our study do not support this hypothesis.

B. 6-DOF Underactuated

This type of kinematics would utilize a haptic interface that has 6-DOF motion but only 3-DOF actuation (alternatively, the kinematics could utilize a haptic interface with 6-DOF actuation wherein the actuators responsible for orientation are simply not activated, as we do in this letter). The most common example of this type of interface is the Geomagic Touch (formerly the PHANTOM Omni). The actuated 3-DOF Cartesian position of the stylus' gimbal (i.e., wrist) is mapped to the 3-DOF Cartesian position of the instrument's end-effector, and the sensed-but-not-actuated rotation about the stylus' axis is mapped to the rotation of the instrument about its shaft axis. This method leaves the 2-DOF "pointing" orientation of the stylus free, as shown in Fig. 2(b); the surgeon can rotate the stylus' unactuated 2-DOF gimbal without any motion of the instrument resulting, which has the potential to lead to confusion. Additionally, the orientation of the stylus in the surgeon's hand will not be aligned with the orientation of the instrument observed in the microscope in general, which could also contribute to confusion. Potential benefits of this type of haptic interface include low cost and compact size. A custom haptic interface was created in [12] that implemented these kinematics.

We originally hypothesized that the 6-DOF Underactuated kinematics would be the worst option due to the disconnect between 6-DOF hand motions and 4-DOF instrument motions. However, as we will show, the results of our study do not support this hypothesis.

C. 4-DOF Separable

This type of kinematics utilizes a haptic interface that is essentially two decoupled interfaces—a 3-DOF Cartesian interface that is mapped to the 3-DOF Cartesian position of the end-effector, and a 1-DOF rotation that is mapped to the 1-DOF rotation about the instrument's shaft axis. Unlike with the 4-DOF Virtual Trocar kinematics, there is no attempt here to align the stylus' 2-DOF pointing orientation with that of the instrument (which we have established cannot be controlled independently of the end-effector's position). This method is motivated by studies that show that translations and rotations are *separable* in the human mind [13], [14]. The potential benefit of this type of haptic interface is that there is a one-to-one mapping between motions of the haptic interface and motions of the instrument, unlike with the 6-DOF Underactuated kinematics, but with the same low cost and compact size of the 6-DOF Underactuated interfaces. However, using this method,

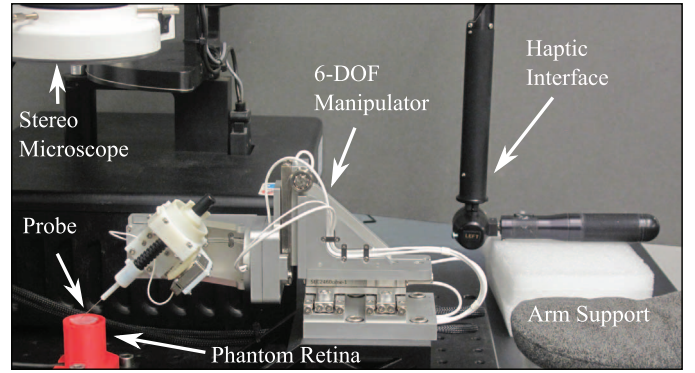


Fig. 3. Experimental setup of the retinal-surgery system. The surgeon looks at the phantom retina using a stereo microscope, and telemanipulates the end-effector of the instrument using the PHANTOM Premium 6DOF haptic interface under different software-controlled kinematics to interact with a force-sensitive phantom retina.

there is not perfect correspondence between the 2-DOF pointing orientation of the stylus in the surgeon's hand and the orientation of the instrument observed in the microscope, which could lead to confusion.

Our group recently implemented such a haptic interface by mechanically locking the gimbal of a Geomagic Touch to eliminate 2-DOF [8], as shown in Fig. 2(c). We used the device to telemanipulate a compact retinal-surgery manipulator. In our experiments, we found that subjects who were inexperienced in real retinal surgery performed better (in certain metrics of success) than expert surgeons who had performed a significant number of real surgeries. Additionally, the expert surgeons complained that the restrained gimbal prevented them from using their own wrist motions efficiently. This led us to question the decision to lock the stylus' gimbal to enforce 4-DOF motion, and ultimately led to the study in this letter.

III. METHODS

A. Subjects

An experiment is performed by 12 (8 male, 4 female) right-handed subjects with ages 23 to 42 years, recruited from the university population with the approval of the institutional review board. Subjects had normal touch sensation and normal (corrected) vision, by self-report, and no prior retinal-surgery experience. Subjects were not compensated.

B. Apparatus

1) *Retinal Manipulator*: The manipulator (Fig. 3), developed in [8], comprises a 3-DOF translation stage and a 3-DOF spherical wrist, which enables the manipulator to position the instrument inside a 20-mm-diameter spherical-section bowl centered on the retina using a virtual RCM located at the trocar on the surface of the eye (which is a sphere of approximately 25.4-mm diameter). The positioning precision of the manipulator while performing constrained motion near the retina is $< 1 \mu\text{m}$, and the maximum velocity at the end-effector is 6 mm/s. Because the manipulator utilizes piezoelectric stick-slip actuators, it effectively behaves as an admittance-type device, only moving when commanded to do so.

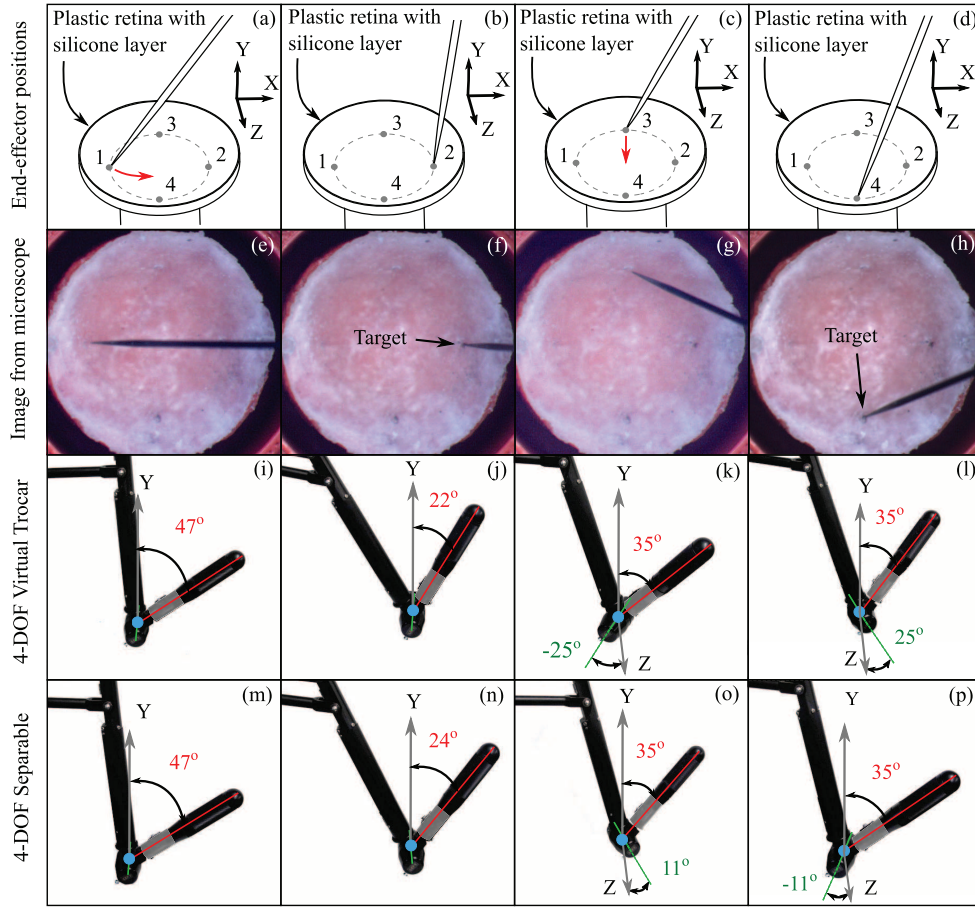


Fig. 4. (a)–(d) Illustration of the end-effector at different target points on the retina. (e)–(h) Microscope image of the phantom retina with the end-effector at different target points as shown in (a)–(d), respectively. The black dots ($\sim 100 \mu\text{m}$) are the target points to which the subjects move the end-effector, labeled in (f) and (h). The haptic-interface stylus orientations are shown in (i)–(l) for the 4-DOF Virtual Trocar kinematics, and in (m)–(p) for the 4-DOF Separable kinematics, for the end-effector positions in (a)–(d), respectively; with the 6-DOF Underactuated kinematics, the orientation of the stylus is controlled by the operator, and hence not shown. The blue dot in the center of the gimbal indicates the point on the haptic interface that is mapped to the end-effector of the manipulator (i.e., the tip of the instrument), and the grey region indicates the gripping area on the stylus.

2) Telemanipulation System: A PHANTOM Premium 6DOF is used as the master haptic interface to telemanipulate the retinal-surgery slave manipulator. A master-slave position controller is implemented in which the scaled slave end-effector position is mapped as a proxy point in the master workspace, and a software spring-damper ($K_p = 0.1 \text{ N/mm}$, $K_d = 0.004 \text{ N} \cdot \text{s/mm}$) is implemented between the proxy and the position of the master haptic interface's gimbal. The scaled position of the master's gimbal is given as a position command to the slave's end-effector. The orientation of the stylus is set according to the haptic-interface kinematics used, as described below. A low-level controller is implemented to servo the end-effector to the desired Cartesian position in its workspace. A clutch (foot pedal) is used to engage/disengage the slave from the master. The RCM movement of the instrument about the trocar is handled in software, and is transparent to the user. A master:slave scaling of 8:1 was chosen such that the task would not require repositioning of the master during a trial. For reference, an 8:1 scaling was used in [8], and a 7:1 scaling was used in [6]. An instrument with a tungsten probe at the tip was used as the end-effector for experiments in this study.

Three different haptic-interface kinematics as described in Section II were implemented in software. Figure 4 shows the orientation of the haptic-interface stylus when the end-effector is at different points on the retina. With the 4-DOF Virtual Trocar kinematics, a trocar point is mapped to the workspace of the haptic interface, and the required orientation of the stylus is calculated based on the trocar point and the end-effector position. A software spring-damper ($K_p = 4000 \text{ N/rad}$, $K_d = 15 \text{ N} \cdot \text{s/rad}$) is implemented on the two master gimbal joints to achieve the desired orientation for the stylus. The result is that the orientation of the stylus matches the orientation of the instrument on the manipulator at each instant as can be seen in Fig. 4(i)–(l). In our experiments, a fixed trocar point is used. With the 6-DOF Underactuated kinematics, the operators are free to rotate the stylus as they wish. With the 4-DOF Separable kinematics, the gimbal joints of the interface are fixed at a constant value relative to the previous link, which simulates a mechanical gimbal lock, using the same gimbal controller gains described above (Fig. 4(m)–(p)). Because of the specific haptic interface used, the orientation of the stylus at points 1 and 2 on the retina are similar with the 4-DOF

Virtual Trocar and 4-DOF Separable kinematics, whereas the orientations are approximately mirrored about the XY plane at points 3 and 4. In all three haptic-interface kinematics, the roll joint on the stylus is locked in software ($K_p = 4000$ N/rad, $K_d = 15$ N · s/rad) since rotation of the instrument about its shaft axis is not relevant for the Cartesian positioning task used in this study.

3) *Phantom Eye*: A phantom eye setup is used to simulate the retina in this study [8]. The setup consists of a plastic retina with the curvature of a 25.4-mm sphere, which is mounted on an ATI Nano17 SI-12-0.12 force/torque sensor (noise $< \pm 4$ mN). A 0.5-mm-thick silicone layer (Dragon Skin 30, Smooth-On Inc.) is attached to the plastic retina to simulate the deformable behavior of a real retina. The stiffness of the silicone layer is different from that of an actual retina, and hence, the forces measured in this study can only be used for comparisons within this study.

C. Procedure

During the experiment, subjects telemanipulated the tip of the tungsten-probe instrument of the retinal manipulator while visualizing the retina through a microscope. The subjects were instructed to hold the stylus of the haptic interface like a pen. In each trial, the subject had to move the end-effector from one point to another on the surface of the retina (Fig. 4(a)–(d)). Trials were performed in the X direction (point 1 to point 2) or the Z direction (point 3 to point 4). At the start of a trial, the end-effector was automatically positioned at the start point (point 1 or 3), and subjects were instructed to move the probe tip to the end point (point 2 or 4, respectively) along a straight line as viewed from above while maintaining contact with the silicone retina. The subjects were instructed to touch the retina as delicately as possible without breaking contact, while drawing as straight a line as possible to the target, and they were instructed to take as much time as necessary to do so. An audio alarm was played when the downward force on the retina was less than 4 mN (the sensor's noise level), indicating the probe tip was not touching the retina sufficiently. Subjects were instructed to note the deformation of the retina as an indication of excessive downward forces.

Ten trials were performed per subject for each combination of direction and haptic-interface kinematics. Six permutations of the order of the three different haptic-interface kinematics are possible, and two subjects perform each particular order. The order in which the two different directions were assigned for a particular haptic-interface kinematics was randomized, and all ten trials for a particular direction were performed together, followed by the next direction. After changing to a new haptic-interface kinematics, subjects were given a 5 min trial period with the new system.

Points 1, 2, 3, and 4 were determined by the experimenter by touching the points on the surface with the probe tip and registering the positions in software before the start of experiments, and were the same for all the subjects. The distance between point 1 and point 2, and point 3 and point 4, was 11 mm. During experiments, the sclera of the model eye [8] was removed after registering the trocar position to provide an unhindered view

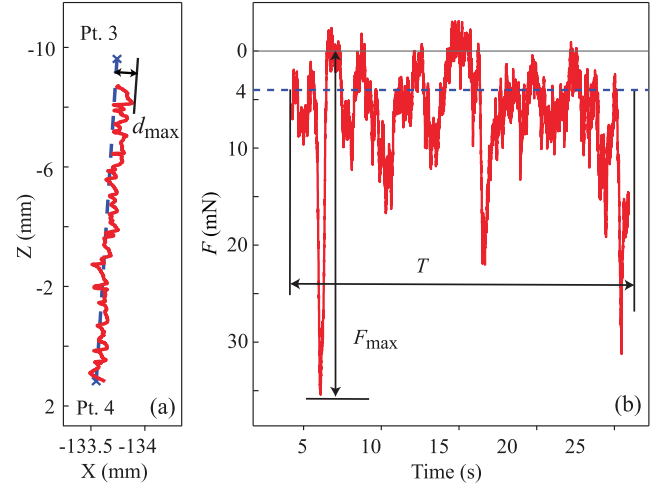


Fig. 5. Typical experimental trial. (a) Position of the probe-tip (solid red line) as the subject telemanipulates it from point 3 to point 4 (blue crosses connected by blue dashed line). (b) Corresponding force data from the phantom retina segmented above and below the threshold force.

of the silicone retina and to eliminate the need for a fiber-optic light source.

At the end of the experiment, subjects were asked to rate the different haptic-interface kinematics in terms of the most comfortable and the least comfortable, and the haptic-interface kinematics in which they thought (subjectively) that their control of the probe tip was best and worst.

D. Measures

To evaluate performance, we use a variety of metrics to quantify the deviation of the probe tip from the desired straight-line path as viewed from above, the ability to follow the curvature of the retina while controlling the forces applied on the retina, and the completion time for a trial. Figure 5(a) and 5(b) shows the path taken by the probe tip and the force data, respectively, during a typical trial in which the subject is telemanipulating the probe tip from point 3 to point 4. Data in a trial was analyzed only after the probe tip moved a distance of 1 mm from the start point.

To measure deviation from the desired straight-line path as viewed from above, we compute the mean deviation (\bar{d}) and the maximum deviation (d_{max}) of the probe tip from a vertical plane passing through the two points of interest (see Fig. 5(a)). A low value for \bar{d} and d_{max} is desirable.

To measure the ability of the subject to follow the curvature of the retina, we use the fraction of the completion time for a trial for which the probe tip is not in contact with the retina (τ_{nc}). Using a force metric is not adequate, as a subject who never touches the retina in a trial will get a perfect score, which does not accurately describe his/her ability to follow the curvature of the retina. The end-effector is considered to be not in contact with the retina if the force magnitude on the retina is less than 4 mN. A value of $\tau_{nc} = 0$ would mean that the subject maintained contact with the retina throughout the trial (never hearing the audio alarm), which would likely be indicative of pressing too hard on the retina (since visual

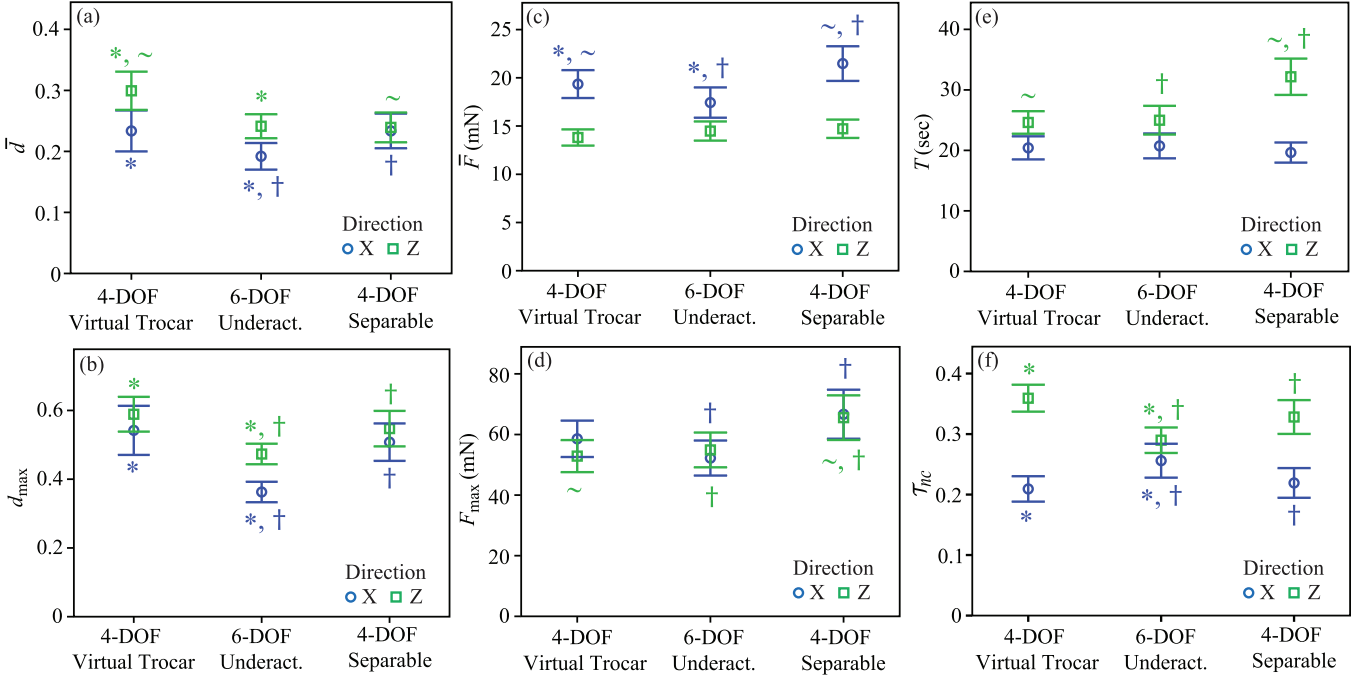


Fig. 6. Experimental results for all subjects and trials for \bar{d} , d_{\max} , \bar{F} , F_{\max} , T , and τ_{nc} for a given haptic-interface kinematics and motion direction. Error bars indicate the 95% confidence interval on the mean. Matching symbols on error bars in a given direction indicate statistically significant differences between two groups. X and Z directions are considered separately.

deformations of the silicone retina happen at forces larger than 4 mN). A value of $\tau_{nc} = 1$ would indicate that the audio alarm was on for the entire trial, indicating that the subject was not maintaining sufficient contact. An ideal subject touching the retina as delicately as possible would have a value of approximately $\tau_{nc} = 0.5$, indicating that the subject could perfectly track the curved retinal surface with a delicate touch, and could respond to the audio alarm appropriately. It would also be possible to have a value $\tau_{nc} = 0.5$ from pushing too hard half of the time and then breaking contact for half of the time, which would be undesirable, but such a scenario would be captured by the downward-force metrics discussed next.

To evaluate the subjects' ability to control downward forces applied on the retina, we look at the mean downward force (\bar{F}) and the maximum downward force (F_{\max}) in a trial (see Fig. 5(b)). Only force magnitudes above the threshold of 4 mN are considered for calculating \bar{F} and F_{\max} . A low value for \bar{F} and F_{\max} is desirable. We also note that τ_{nc} should be taken into account when evaluating force results (e.g., a seemingly good mean force could result from poor contact being maintained).

Finally, we look at the total completion time (T) for a trial. Although subjects were instructed to take as much time as required to complete a trial, the completion time gives us information about the intuitiveness of the different haptic-interface kinematics.

IV. RESULTS

Figure 6 shows the experimental results for all conditions and subjects. We find a strong effect of the direction of the motion of the probe tip (X vs. Z), so the results for each direction are analyzed separately. An independent-samples t-test was used to

compare the different kinematics, using a significance level of $\alpha < 0.05$.

A. Ability to Follow a Desired Path

We find that the mean deviation from a straight path as viewed from above (\bar{d}) is significantly higher with the 4-DOF Virtual Trocar kinematics than with both of the others for motions in the Z direction (Fig. 6(a)). \bar{d} is significantly lower with the 6-DOF Underactuated kinematics than with both of the others for motions in the X direction. We find that the maximum deviation from the straight path (d_{\max}) is significantly lower with the 6-DOF Underactuated kinematics than with both of the others for motions in both the X and Z directions.

We find that the fraction of time for which the end-effector is not in contact with the retina (τ_{nc}) is significantly lower (i.e., farther from 0.5) with the 6-DOF Underactuated kinematics than with both of the others for motions in the Z direction (Fig. 6(f)). However, τ_{nc} is significantly higher (i.e., closer to 0.5) with the 6-DOF Underactuated kinematics than with both of the others for motions in the X direction, and it appears that it is in this direction that subjects have the most difficulty following the curved retinal surface (based on this metric).

B. Force Applied to the Retina

We find that the mean downward force on the retina (\bar{F}) is significantly lower with the 6-DOF Underactuated kinematics than with the 4-DOF Virtual Trocar kinematics, which is in turn significantly lower than with the 4-DOF Separable kinematics for motions in the X direction (Fig. 6(c)). We find that the maximum downward force on the retina (F_{\max}) is significantly higher with the 4-DOF Separable kinematics than with both of

the others for motions in the Z direction. F_{\max} is significantly higher with the 4-DOF Separable kinematics than with the 6-DOF Underactuated kinematics in the X direction (Fig. 6(d)). We also note that the maximum forces are an order of magnitude larger than the sensor's noise. By looking at these results together, we find that the 6-DOF Underactuated kinematics leads to the best performance in terms of being able to precisely control (and limit) the force applied to the retina, and the 4-DOF Separable kinematics leads to the worst performance.

C. Completion Time

We find that the completion time (T) for motions in the Z direction is significantly higher with the 4-DOF Separable kinematics than with both of the others (Fig. 6(e)). From this alone, we conclude that the 4-DOF Separable kinematics are the worst in terms of completion time.

D. Qualitative Assessment of Different Kinematics

The majority of subjects found the 6-DOF Underactuated kinematics to be the most comfortable to use (92%) and believed that they had best control of the end-effector with these kinematics (58%). The majority of subjects found the 4-DOF Virtual Trocar kinematics to be the least comfortable to use (58%) and believed these kinematics resulted in the worst control over the end-effector (67%). The qualitative surveys clearly point to the 6-DOF Underactuated kinematics being the most preferred, and the 4-DOF Virtual Trocar being the least preferred.

V. DISCUSSION

Each of our performance metrics when considered individually is an imperfect measure, but by looking at the results for \bar{d} , d_{\max} , and τ_{nc} from Section IV-A in their totality, we conclude that the 6-DOF Underactuated kinematics leads to the best overall performance in terms of being able to precisely control the end-effector of the instrument along a desired path on the surface of the retina. When we combine that conclusion with the results for applied force, completion time, and qualitative assessment, we can make an overall conclusion for our study. We find that for a task that is reminiscent of tracing the surface of the retina while applying a gentle force—a skill that is important for nearly all retinal-surgery procedures—the subjects' performance was best overall with the 6-DOF Underactuated kinematics, and the subjects also preferred these kinematics over the others considered. For motions in the X direction, the superiority of the 6-DOF Underactuated kinematics is absolutely conclusive: the time in contact with the retina is the most (that is, the best, since it is the closest to 0.5) even as the average force is the lowest of all kinematic types; the completion time is the same across types, removing the possibility of that being a confounding factor; at the same time, the deviation from a straight path as viewed top-down from the microscope is the smallest, both in terms of the mean and the maximum, for this kinematic type. After the 6-DOF Underactuated kinematics, subjects' performance was

best with the 4-DOF Virtual Trocar kinematics; however, subjects subjectively preferred these kinematics the least of the three considered.

The hand motions required (and permitted) with the three haptic-interface kinematics are quite different from each other. With the 4-DOF Virtual Trocar, the subjects use coupled translations and rotations of the hand/wrist to move the stylus such that the orientation constraint on the stylus due to a fixed trocar point was satisfied. With the 6-DOF Underactuated kinematics, it was observed that the subjects typically used wrist rotations to move the stylus, as the orientation of the stylus is set by the subject as desired. With the 4-DOF Separable kinematics, the subjects had to largely use translations of the hand to move the stylus. This difference in the type of motion required by the subjects likely explains the degraded performance with the 4-DOF Separable kinematics, as maintaining precision while using translation hand movements (i.e., arm movements) is difficult. Due to the kinematic similarity between the 4-DOF Virtual Trocar and 4-DOF Separable kinematics in the X direction, they show similar performance across metrics in the X direction, as expected.

In our study, we found a strong dependence of our metrics on the direction of motion of the probe tip (X vs. Z). It could be possible that the joint mechanics and asymmetric force/torque characteristics of the Phantom Premium 6DOF resulted in such a behavior. However, our results are independent of the direction of motion, and are not affected by the dependence of the metrics on the direction of motion.

In our study, the 4-DOF Virtual Trocar kinematics were implemented in software using a fully actuated PHANTOM Premium 6DOF haptic interface. We must be cautious that our results may be affected by that implementation, and may not apply directly to custom 4-DOF Virtual Trocar interfaces that implement the kinematics mechanically. In a software implementation, end-effector motions require simultaneous translation and rotation motions of the stylus. Because the haptic interface used in this study is an impedance-type device, the orientation constraint on the stylus has limited stiffness. Any error in the orientation between the stylus and the desired orientation will cause a restoring torque on the stylus opposing the movement of the stylus by the subject away from the desired orientation. For instance, if the subject attempts to move the stylus with a pure translation, without permitting the controller to properly orient the stylus, a torque will be applied on the stylus to reduce its orientation error. Alternatively, if the subject attempts to use mainly rotary motion of the stylus, like observed with the 6-DOF Underactuated kinematics, a restoring torque will be applied against the pure rotary motion of the stylus induced by the subject. This effect is pronounced if minimal master-slave scaling is implemented, since a small translation of the end-effector (and thus the stylus) corresponds to a relatively large change in instrument (and thus stylus) orientation, which can result in large restoring torques. For the 8:1 master-slave scaling used in this study, the restoring torques seemed negligible. We believe that the combined effect of the restoring torques and the complexity of movement required with the 4-DOF Virtual Trocar kinematics contributed to the low scores in its subjective qualitative assessment. It is possible that a

haptic device that is capable of rendering stiffer environments could lead to better outcomes with the 4-DOF Virtual Trocar kinematics implemented in software. Because of limitations on the maximum stiffness that can be rendered by haptic devices, results for the 4-DOF Virtual Trocar kinematics should be used with caution when comparing haptic devices with a physical trocar.

It should be noted that the subjects in our study were surgically inexperienced, and the outcomes, in terms of the objective and subjective metrics, could be different for experienced retinal surgeons. However, we expect that with limited training, experienced surgeons should be able to perform optimally with the haptic-interface kinematics that was found to provide optimal performance for inexperienced subjects. As a single data point, the experienced-surgeon co-author of this letter has a subjective preference that agrees with the results of this study.

Until this point, we have neglected an important component of retinal surgery: orbital manipulation. During retinal surgery, surgeons often rotate the eye (under the stationary microscope) to better visualize a specific location on the retina, and then perform precision tasks at that new location. This is accomplished by using the two instruments, acting in concert, to apply forces on the trocars. So although the instrument movements considered in this letter were only 4-DOF, a surgeon utilizes the full 6-DOF pose of an instrument to perform retinal surgery (2-DOF for orbital manipulation, and 4-DOF for movement within the eye). This means that any retinal-surgery robot should also be capable of manipulating the 6-DOF pose of the instrument, if orbital manipulation is required. However, this does not necessarily mean that the master haptic interface in a telemanipulated retinal-surgery system must have 6-DOF. If the intent is to recreate the method of manual orbital manipulation at the master, the most obvious way to accomplish it is using a 6-DOF fully actuated haptic interface, such as the PHANTOM Premium 6DOF used in this letter. It would be difficult to recreate manual orbital manipulation using a 6-DOF Underactuated haptic interface, such as a Geomagic Touch, since it is not possible to render trocar forces to the stylus and it is not possible to enforce coordination of the styluses of the left and right hands. However, one could imagine methods in which orbital manipulation could be accomplished in a telemanipulation scenario that do not attempt to recreate the haptics of manual orbital manipulation—methods that could be implemented with 6-DOF Underactuated interfaces or custom 4-DOF interfaces—using clutching techniques that decouple orbital manipulation from precision instrument motions. In any case, the results of the study in this letter should be considered not only in determining the type of haptic interface to use in a retinal-surgery telemanipulation system, but also how that interface is controlled during tasks that require high precision.

VI. CONCLUSIONS

We have studied operator performance during a task reminiscent of telemanipulated retinal surgery with three differ-

ent haptic-interface kinematics implemented in software on a PHANTOM Premium 6DOF haptic interface. An instrument attached to a retinal-surgery manipulator was telemanipulated to perform a precise positioning task on a force-sensing phantom retina; the task and metrics were designed to capture a range of skills important during actual retinal surgery. Results from a study with 12 novice human subjects show that the subjects' overall performance was best, in terms of the ability to precisely and quickly trace a desired path on the curved surface of the retina while applying gentle forces, with the kinematics that represent a compact, inexpensive, and commercially available option, and that subjects' subjective preference agrees with the objective performance results. It was noted that the results of this study may not translate directly to experienced surgeons, who may have pre-existing biases due to their specialized training, without additional training.

REFERENCES

- [1] J. R. Wilkins *et al.*, "Characterization of epiretinal membranes using optical coherence tomography," *Ophthalmology*, vol. 103, no. 12, pp. 2142–2151, 1996.
- [2] P. S. Jensen, K. W. Grace, R. Attariwala, J. E. Colgate, and M. R. Glucksberg, "Toward robot-assisted vascular microsurgery in the retina," *Graefes Arch. Clin. Exp. Ophthalmol.*, vol. 235, no. 11, pp. 696–701, 1997.
- [3] W. Wei, R. Goldman, N. Simaan, H. Fine, and S. Chang, "Design and theoretical evaluation of micro-surgical manipulators for orbital manipulation and intraocular dexterity," in *Proc. IEEE Int. Conf. Robot. Autom.*, 2007, pp. 3389–3395.
- [4] Y. Ida, N. Sugita, T. Ueta, Y. Tamaki, K. Tanimoto, and M. Mitsuishi, "Microsurgical robotic system for vitreoretinal surgery," *Int. J. Comput. Assisted Radiol. Surg.*, vol. 7, no. 1, pp. 27–34, 2012.
- [5] M. Nasser *et al.*, "The introduction of a new robot for assistance in ophthalmic surgery," in *Proc. Int. Conf. IEEE Eng. Med. Biol. Soc.*, 2013, pp. 5682–5685.
- [6] H. Meenink *et al.*, "Robot-assisted vitreoretinal surgery," *Med. Robot. Minimally Invasive Surg.*, pp. 185–209, 2012.
- [7] A. Gijbels, E. Vander Poorten, P. Stalmans, H. Van Brussel, and D. Reynaerts, "Design of a teleoperated robotic system for retinal surgery," in *Proc. IEEE Int. Conf. Robot. Autom.*, May 2014, pp. 2357–2363.
- [8] M. Nambi, P. S. Bernstein, and J. J. Abbott, "A compact retinal-surgery telemanipulator that uses disposable instruments," in *Medical Image Computing and Computer-Assisted Intervention*, N. Navab, J. Hornegger, W. M. Wells, and A. F. Frangi, Eds. New York, NY, USA: Springer, 2015, pp. 258–265.
- [9] A. Uneri, M. A. Balicki, J. Handa, P. Gehlbach, R. H. Taylor, and I. Iordachita, "New steady-hand eye robot with micro-force sensing for vitreoretinal surgery," in *Proc. IEEE Int. Conf. Biomed. Robot. Biomechatronics*, 2010, pp. 814–819.
- [10] A. Gijbels, E. Vander Poorten, B. Gorissen, A. Devreker, P. Stalmans, and D. Reynaerts, "Experimental validation of a robotic comanipulation and telemanipulation system for retinal surgery," in *Proc. IEEE Int. Conf. Biomed. Robot. Biomechatronics*, 2014, pp. 144–150.
- [11] R. Hendrix, N. Rosielle, and H. Nijmeijer, "Design of a haptic master interface for robotically assisted vitreo-retinal eye surgery," in *Proc. Int. Conf. Adv. Robot.*, 2009, pp. 1–6.
- [12] H. Takahashi *et al.*, "Master manipulator with higher operability designed for micro neuro surgical system," in *Proc. IEEE Int. Conf. Robot. Autom.*, 2008, pp. 3902–3907.
- [13] M. R. Masliah and P. Milgram, "Measuring the allocation of control in a 6 degree-of-freedom docking experiment," in *Proc. SIGCHI Conf. Human Factors Comput. Syst.*, 2000, pp. 25–32.
- [14] R. J. K. Jacob, L. E. Sibert, D. C. McFarlane, and M. P. Mullen Jr., "Integrality and separability of input devices," *ACM Trans. Comput. Human Interact.*, vol. 1, no. 1, pp. 3–26, 1994.